Available online at www.sciencedirect.com
SCIENCE DIRECT®

Journal of the European Ceramic Society 24 (2004) 1295–1299

www.elsevier.com/locate/jeurceramsoc

Phases investigation in the antimony doped Bi_2O_3 system

V. Fruth[a,*], M. Popa[b], D. Berger[c], C.M. Ionica[a], M. Jitianu[a]

[a]*Romanian Academy, Institute of Physical Chemistry, Spl. Independentei 202, Bucharest 77208, Romania*
[b]*Tokyo Institute of Technology, Materials and Structures Laboratory, Nagasuta 4259, Midori-ku, Yokohama 226-8503, Japan*
[c]*Department of Inorganic Chemistry, University "Politehnica" Bucharest, str. Polizu 1, Bucharest, Ro-78126, Romania*

Abstract

The present study investigates the influence of Sb ions, introduced as dopants in α-Bi_2O_3, on the structure of the oxide polymorph forms obtained at high temperature. The structural changes of α-Bi_2O_3 for compositions in the system $Bi_{2-x}Sb_xO_3$ ($x = 0$, 0.05, 0.1, 0.15, 0.2), at different thermal treatment temperatures were analyzed by thermal analysis, powder X-ray diffraction and infrared transmission spectroscopy. A tendency of the structure to change to a higher symmetry (monoclinic → tetragonal → cubic) was observed, as the content in antimony increased and the temperature reached 850 °C. The presence of Sb_2O_3 in the Bi_2O_3 oxide system promotes an oxygen release from the oxide and enlarges the stabilization domain of the δ-phase.

Keywords: Bismuth oxides; Polymorph forms; Sb_2O_3 dopant

1. Introduction

Oxide ion conductors have been increasingly studied for many years because of their application in many devices with high economical interest such as solid oxide fuel cells (SOFC), oxygen sensors, dense ceramic membranes for oxygen separation, membrane reactors for oxidative catalysis.[1–3]

In order to favor high oxide ion mobility Boivin[4] defined some basic requirements: (i) the existence of a supernumerary number of equivalent crystallographic sites for oxide oxygen ions, criteria which can be naturally satisfied. For instance, the δ form of Bi_2O_3 exhibits the fluorite-type sesquioxide lattice, same structure as the doped zirconia but contains 25% of naturally unoccupied oxygen sites. However, because of the very large number of vacancies, long-range order easily occurs at low temperature and, on cooling, the material undergoes a phase transition accompanied by a dramatic three orders of magnitude lowering of its conductivity. Substitution for Bi^{3+} by another cation can prevent long-range ordering being established on cooling; (ii) the energy equivalence criteria between many oxygen sites is more easily satisfied when the crystal lattice belongs to a higher symmetry system. However, some materials exhibit very high conductivity despite a non-cubic symmetry (the conductivity is strongly anisotropic—e.g. the BIMEVOX phases); (iii) the polarisability of the cation host structure. In order to jump from one site to the next available one, the oxygen ion must cross a bottleneck usually delimited by three cations. Polarisable cations will make this crossing very much easier. Moreover, an additional effect can occur if the cation polarisability results from the presence of active electron lone pairs (Bi^{3+}, Sb^{3+}, Pb^{2+}, Sn^{2+}, Tl^{+}...). In that case, a dynamic accompaniment of the anion jump can exalt the mobility. Owing to those requirements, fast oxide conductors adopt a limited number of structures.

Doped bismuth oxide systems exhibit a complex array of structures depending on the dopant concentration. The aim of this article is to investigate the influence of an isoelectronic ion as antimony on the polymorph transition of Bi_2O_3.

2. Experimental procedure

Bi_2O_3 (99%) and Sb_2O_3 (99%) were mixed in stoichiometrc proportions to form $(Bi_2O_3)_{2-x}(Sb_2O_3)_x$ ($x = 0$, 0.05, 0.1, 0.15, 0.2). The samples were repeatedly ground in a mortar and pestle to remove any present agglomerates, then pressed into discs of 10 mm diameter

* Corresponding author. Tel.: +00 4021 2278895/26; fax: +00 4021 3121147.
E-mail address: vfruth@icf.ro (V. Fruth).

0955-2219/$ - see front matter © 2003 Elsevier Ltd. All rights reserved.
doi:10.1016/S0955-2219(03)00506-5

and sintered at different temperatures up to 850 °C and cooled in the furnace till room temperature.

The structure of the obtained materials was determined by X-ray diffraction (XRD). The XRD patterns were recorded with a standard D5000 Siemens Diffractometer θ–2θ equipped with a graphite monochromatized using Cu K_α radiation ($\lambda = 1.5405$ Å) operating at 40 mA and 40 kV. The IR spectra were recorded using a Specord M80 type Carl Zeiss Jena spectrometer in the spectral range 800–200 cm^{-1}. Thermal analysis (DTA/TG) was realized with a MOM-OD 102 derivatograph, in non-isothermal conditions, in air. More detailed thermal analysis was performed in a Stanton thermobalance, with sensibility 0.1 mg. The powder morphology was determined by scanning electron microscopy with a Scanning microscope Zeiss DSM 942 equipped with a Link Energy Dispersive X-ray system.

3. Results and discussions

The thermal analysis results for the starting powders mixtures, presented in detail in a prewious paper[5] showed for all Sb-doped samples a small exothermal event at 500 °C, associated with the oxidation of Sb^{3+}–Sb^{5+}; in the temperature range of 520–560 °C, TG curves recorded a weigh loss of 1.5–2% associated with an endothermic event on the DTA curves, except for Sb-free samples. A high content in Sb_2O_3 decreased the transition temperature $\alpha \rightarrow \delta$ (735–710 °C) and increased the melting point from 835 to 880 °C.

The thermal behavior of the samples after annealing treatment was examined. The color of the powders changed from deep orange to yellow as the content in Sb_2O_3 increased. Fig. 1a shows the DTA curves of the annealed samples at 800 °C for 20 h. Two small endothermic events are present in the range 630–655 °C. The temperature corresponding to the transition $\alpha \rightarrow \delta$ Bi_2O_3 was noticed at ~730 °C and the melting of the samples took place at ~880 °C, at higher temperature than the undoped sample. The melt crystallized at 822 °C in the case of Sb-free samples and at 790–795 °C for the Sb_2O_3 containing samples (Fig. 1b). The $\delta \rightarrow \alpha$ Bi_2O_3 transition was assigned to the observed exothermal event at 660 °C (Bi_2O_3 curve). When antimony is present, small exothermal events were observed in the range 630–550 °C. A higher content in Sb lowers the crystallization process of the metastable phases identified in the sample. No changes were observed on the TG curves.

The phases identified by X-ray diffraction after different treatments are presented in Table 1. All the samples contained phases mixture, mainly the tetragonal $\beta^*Bi_2O_3$ and cubic $\gamma^*Bi_2O_3$ phases. Gattow and Schroeder[6] proposed that the impurity forms of the β-, γ- and δ- polymorphs be expressed using star designa-

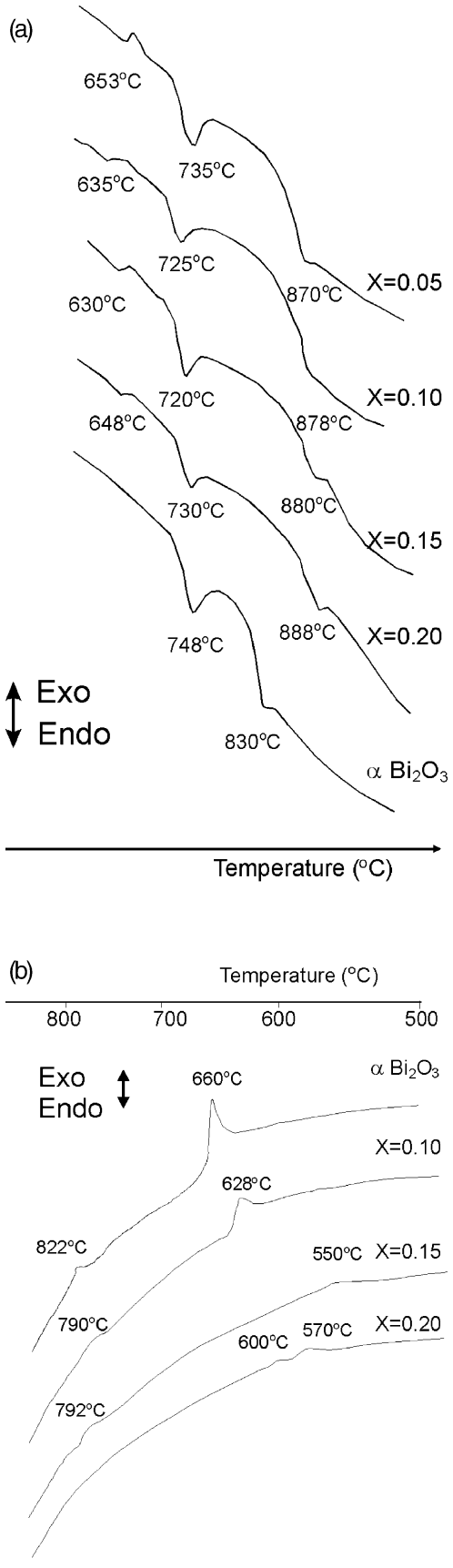

Fig. 1. DTA curves of the $Bi_{2-x}Sb_xO_3$ (x = 0–0.20) mixtures after 20 h annealing treatment at 800 °C; (a) heating, (b) cooling.

tion (e.g. β*, γ*, δ*). The phases were identified using JCPDS cards 45-1344, 74-1375, 74-1373, 48-0469). Short annealing treatments at temperatures as low as 600 °C, produced no transition of the monoclinic αBi_2O_3 phase, but some incipient crystallization peaks of the tetragonal phase were observed. This phenomenon may be considered a surface (interface) effect. At 760 °C, after 10 h treatment the promotion of the tetrahedral and cubic phases becomes evident as the content in antimony increases. This tendency was noted also at higher temperature, as can be confirmed by the results showed in Fig. 2. As the temperature increased and the concentration in antimony was greater, the cubic phase became dominant. Some of the reflections can be attributed to a $\delta^*Bi_2O_3$ phase. αSb_2O_4 was also identified in the samples. At higher concentration of antimony (x = 0.8) and 850 °C the compound $BiSbO_4$ was obtained mixed with $\gamma^*Bi_2O_3$ phase. This infers an

Table 1
Phases identified in the sample after specified annealing treatments

Sample	Phases identified in the annealed sample				
	600 °C/5 h	760 °C/10 h	800 °C/20 h	820 °C/20 h	850 °C/40 h
BS1 (x = 0.05)	αBi_2O_3	α Bi_2O_3 β* Bi_2O_3	α Bi_2O_3 β* Bi_2O_3	α Bi_2O_3 β* Bi_2O_3	γ*Bi_2O_3, β*Bi_2O_3 δ*Bi_2O_3
BS2 (x = 0.10)	αBi_2O_3 β*Bi_2O_3 trace)	β* Bi_2O_3 α Bi_2O_3	β*Bi_2O_3 γ* Bi_2O_3	β*Bi_2O_3 γ* Bi_2O_3	γ*Bi_2O_3↑ β*Bi_2O_3↓
BS3 (x = 0.15)	αBi_2O_3 β*Bi_2O_3(trace)	β*Bi_2O_3 γ*Bi_2O_3 αSb_2O_4	γ* Bi_2O_3 β* Bi_2O_3		γ*Bi_2O_3↑ β*Bi_2O_3↓ αSb_2O_4
BS4 (x = 0.20)	αBi_2O_3 β*Bi_2O_3(trace)	γ*Bi_2O_3 β*Bi_2O_3 αSb_2O_4	γ*Bi_2O_3 β* Bi_2O_3		γ*Bi_2O_3↑ δ*Bi_2O_3↓, αSb_2O_4
BS5 = 0.40) BS6 = 0.80)					γ*Bi_2O_3↓,αSb_2O_4 $BiSbO_4$,γ*Bi_2O_3↓

↑↓—Tendency of crystallization.

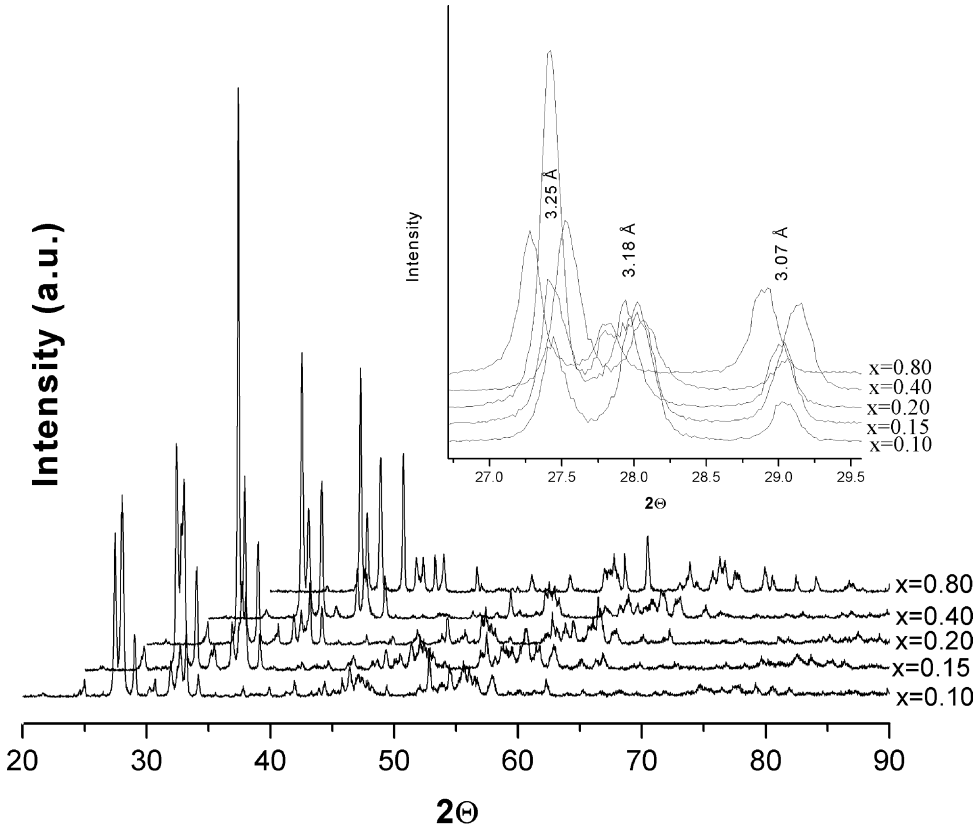

Fig. 2. XRD patterns of the $Bi_{2-x}Sb_xO_3$ (x = 0.10–0.80) mixtures after 40 h annealing treatment at 850 °C.

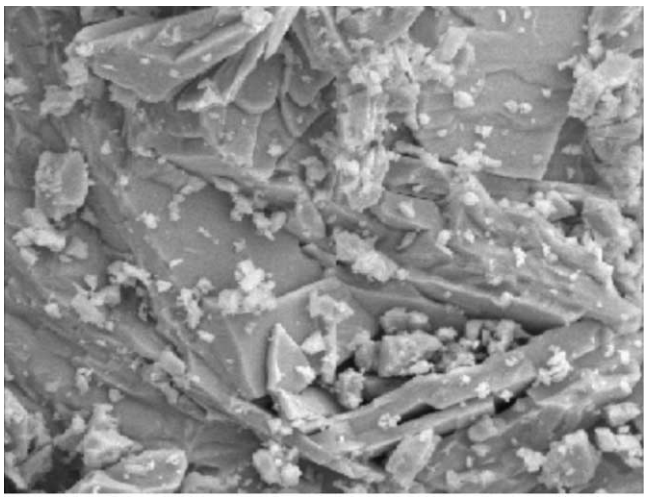

Fig. 3. The SEM micrograph showing the morphology of the powders of composition BS4; x = 0.20 in the system $(Bi_2O_3)_{2-x}(Sb_2O_3)_x$, 850 °C/40 h.

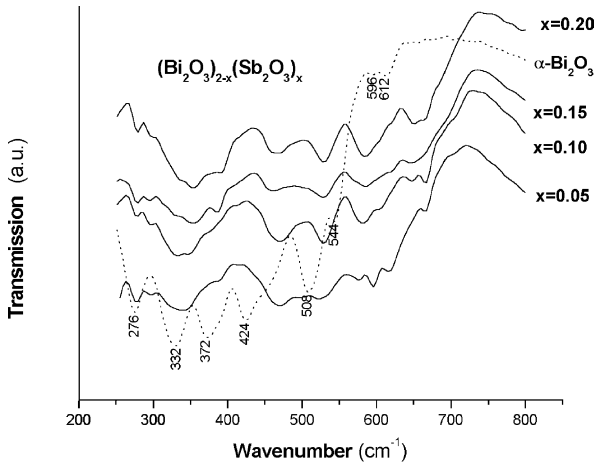

Fig. 4. Infrared spectra of the annealed samples at 850 °C/40 h. (αBi_2O_3 dotted line).

upper limit of the solubility of antimony, which is in agreement with previous reported results by Béqué[7] who established that Bi:Sb 1.1:0.9 ratio represent the upper limit of the solid solution $Bi_{2-x}Sb_xMoO_6$.

The cubic $\gamma^*Bi_2O_3$ phase [Space Group I23 (197)] is actually a mixture of phases with the *a* cell parameter in the range 10.08–10.26 Å. Reportedly, the cell dimensions for $\gamma^*Bi_2O_3$ vary from 10.09 to 10.25 Å for different impurities.[8] These values were influenced by the content in antimony and the annealing temperature. That infers a substitution of the Bi^{3+} ion with the ionic radius of 1.17 Å (CN6), by the smaller ion Sb^{3+} with ionic radius 0.90 Å (CN6).[9]

The SEM/EDX analysis of the samples treated at 850 °C showed similar microstructures with two main detected phases, $\gamma^*Bi_2O_3$ and αSb_2O_4. A general image is shown in Fig. 3 for the composition BS4 (x = 0.20).

Detailed infrared (IR) spectra have been obtained for the annealed compositions $Bi_{2-x}Sb_xO_3$ at room temperature. The spectra are in great concordance with the XRD observations. In the case of bismuth sesquioxide the large distortion of the Bi-O polyhedra for α-Bi_2O_3 separated the Bi-O stretching modes into more localized and narrow-line vibrations. The structure of α-Bi_2O_3 is very complex, two distinct Bi-O polyhedra highly distorted, with bond lengths ranging from 2.08 to 3.25Å being noticed.[10] The differences in the bond lengths in Bi_2O_3 led to different absorption bands, so it can be assumed that the observed fine structure bands can be correlated with the clusters of similar bond lengths. More explicitly, each absorption band found in the range 800–200 cm^{-1} can be correlated with the stretching mode vibration of each type of Bi-O bond, taking into account the intensity and the mean wavenumber of the bands.[10] The characteristic vibrations of the monoclinic Bi_2O_3 structure are slightly shifted and, more significantly, new absorption bands are observed for all the Sb-doped samples at wavenumber greater than 600 cm^{-1} (Fig. 4). The broadness and band contours can be postulated as being due to the particle size and Fröhlich surface mode effect that typically modifies IR spectra of polar compounds,[11] observations supported by XRD analysis. The monoclinic α-Bi_2O_3 was detected in all the samples heated 5 h at 600 °C but a systematic shift of the bands to a higher wavenumber was observed, suggesting a possible substitution of Bi^{3+} by the smaller ions of Sb^{3+}. Sb^{3+} ion enters into the bismuth layer, due to its similar stencil behavior, by the presence of a 5s(2) lone pair associated with Sb^{3+} and 6s(2) associated with Bi^{3+}.[11] The IR spectra of the samples annealed at different temperatures show that the bands identified in the case of samples annealed at 850 °C are broader that those found at 760 °C. The increasing content of antimony in the samples from x = 0.05 – 0.20 led to different features in the IR spectra. It can be concluded that the broad envelope in the metal-oxygen stretching region in the IR spectra of the doped phases can be associated with highly polar bonds and a large longitudinal transverse mode separation.

4. Conclusions

Detailed structural analysis were realized for the system $(Bi_2O_3)_{1-x}(Sb_2O_3)_x$, x = 0.05–0.2. After thermal treatment, all samples contained a phase mixture of $\beta^*Bi_2O_3$ and $\gamma^*Bi_2O_3$ tetragonal and respectively cubic. As the content in antimony increased and the annealing temperature reached 850 °C a transition tendency of the structure to change from lower symmetry to higher symmetry (monoclinic→tetragonal→cubic) was observed, result confirmed both by IR and XRD analysis. The changes in the IR spectra were determined both by oxygen loss of Bi_2O_3 and the beginning of a new network

arrangement characteristic for metastable polymorph Bi_2O_3 forms. The changes in the network arrangements are more evident together with the increase of the Sb content of the samples and the increasing temperature of the thermal treatments.

References

1. Kinne, M., Bernhardt, T. M., Kaiser, B. and Rademann, K., Formation and stability of antimony and bismuth oxide clusters: a mass spectrometric investigation. *Int. J. Mass Spectr. Ion Processes*, 1997, **167/168**, 161–172.
2. Sammes, N. M., Fee, M., Phillips, M. G. and Ratnaraj, R. J, Improved mechanical properties of bismuth lead oxide. *J. Mater. Sc. Let*, 1994, **13**(19), 1395–1396.
3. Ling, C. D., Thompson, J. G., Withers, R. L. and Schmid, S., Synthesis and structural Characterization of a new Family of layered intergrowth phases based on antimony (III) oxide. *J. Solid State Chem.*, 1996, **125**, 19–29.
4. Boivin, J. C., Structural and electrochemical features of fast oxide ion conductors. *Int. J. Inorg. Mater.*, 2001, **3**, 1261–1266.
5. Fruth V., Tanase G., Szatvanyi A. and Berger D., Influence of the Sb_2O_3 on the polymorphism of Bi_2O_3, *International Conference on Materials Science and Engeneering*, Brasov-Romania, vol. IV (2001) 42-48.
6. Gattow, G. and Schroeder, H., Bismuth Oxides: III. *Z. Anorg. Allg. Chem.*, 1962, **318**, 176–189.
7. Béqué, P., Enjalbart, R. and Castro, A., The upper limit of the solid solution $Bi_{2-x}Sb_xMoO_6$. Structure refinment of $Bi_{1.1}Sb_{0.9}MoO_6$. *J. Solid State Chem.*, 2001, **159**, 72–79.
8. Medernach, J. W. and Snyder, R. L., Powder diffraction patterns and structures of bismuth oxides. *J. Am. Ceram. Soc.*, 1978, **61**, 494–497.
9. Shannon, R. D., *Ionic Radii. Acta Cryst.*, 1976, **A32**, 751–767.
10. Betsch, R. J. and White, W. B., Vibrational spectra of bismuth oxide and the sillenite-structure bismuth oxide derivatives. *Spectrochim. Acta*, 1979, **34A**, 505–514.
11. Sammes, N. M., Tompsett, G. and Cartner, A. M., Characterization of bismuth lead oxide by vibrational spectroscopy. *J. Mater. Sci.*, 1995, **30**, 4299–4308.